How alpha beta T cells deal with induced TCR ablation

Polić, Bojan; Kunkel, D.; Scheffold, A.; Rajewsky, K.

Source / Izvornik: **Proceedings of the National Academy of Sciences, 2001, 98, 8744 - 8749**

Journal article, Published version
Rad u časopisu, Objavljena verzija rada (izdavačev PDF)

https://doi.org/10.1073/pnas.141218898

Permanent link / Trajna poveznica: https://urn.nsk.hr/urn:nbn:hr:184:477586

How $\alpha\beta$ T cells deal with induced TCRα ablation

Bojan Polic*†‡, Desiree Kunkel§, Alexander Scheffold§, and Klaus Rajewsky*‡

*Department of Immunology, Institute for Genetics, University of Cologne, Weyertal 121, 50931 Cologne, Germany; §Immunocytometry Group, Deutsches Rheuma–Forschungszentrum Berlin, Schumannstrasse 21/22, 10117 Berlin, Germany; and †Department of Histology and Embryology, Medical Faculty, University of Rijeka, B. Branchetta 20, 51000 Rijeka, Croatia

Contributed by Klaus Rajewsky, May 2, 2001

On deletion of the gene encoding the constant region of the T cell antigen receptor (TCR)α chain in mature T cells by induced Cre-mediated recombination, the cells lose most of their TCR from the cell surface within 7–10 days, but minute amounts of surface-bound TCRβ chains are retained for long periods of time. In a situation in which cellular influx from the thymus is blocked, TCR-deficient naïve T cells decay over time, the decay rates being faster for CD8$^+$ cells ($t_{1/2} \approx 16$ days) than for CD4$^+$ cells ($t_{1/2} \approx 46$ days). TCR$^+$ naïve cells are either maintained (CD8$^+$) or decay more slowly (CD4$^+$; $t_{1/2} \approx 78$ days.) Numbers of TCR-deficient memory T cells decline very slowly (CD8$^+$ cells; $t_{1/2} \approx 52$ days) or not at all (CD4$^+$ cells), but at the population level, these cells fail to expand as their TCR$^+$ counterparts do. Together with earlier data on T cell maintenance in environments lacking appropriate major histocompatibility complex antigens, these data argue against the possibility that spontaneous ligand-independent signaling by the $\alpha\beta$TCR contributes significantly to T-cell homeostasis.

The development of both B and T lymphocytes is governed by the rule that only cells that are able to express a functional antigen receptor [B cell antigen receptor (BCR) and T cell antigen receptor (TCR), respectively) reach the peripheral immune system. However, even beyond the phase of development, antigen receptor expression appears to be of vital importance for the cells. For B lymphocytes, this became apparent in an experiment in which the BCR was ablated on mature cells by conditional gene targeting. This led to rapid apoptosis of the receptorless cells (1). In the case of $\alpha\beta$T cells, mature cells were exposed to an environment in which the major histocompatibility complex (MHC) proteins were absent for whose recognition the cells had been selected during thymic development. In this situation, naive T cells exhibited reduced life spans compared with peripheral T cells in normal physiology (2–7). However, memory T cells appear to depend much less (7) or not at all (6, 8, 9) on recognition of MHC molecules.

Although both types of experiments point to an essential role of the antigen receptor in the maintenance of lymphocytes *in vivo*, they are different in nature and may address different issues. Thus, in the case of B cells, expression of the BCR as such may be required for cellular survival, and it remains unresolved whether recognition of an external ligand is (also) involved. The latter, in turn, seems required for T cell maintenance, but here the possibility remains that a TCR-autonomous maintenance signal also contributes to survival. This could explain why B cells appear to die more rapidly on BCR ablation than T cells in the absence of the appropriate MHC antigens in their environment.

To obtain further insights into these matters, we have now generated an experimental system that allows the inducible ablation of the TCR on mature T cells *in vivo* by Cre recombinase-mediated TCR Cα gene deletion.

Materials and Methods

Mice. The following mouse strains and mutants were used in this study: C57BL/6, TCR Cα^{fl}, Mx-Cre (10), TCR$\alpha^{-/-}$ (11), Rag1$^{-/-}$ (12). Mice were bred and maintained under specific pathogen-free conditions and were used for experiments at the age of 2–4 months. Genotypes were determined by PCR and Southern blot analysis by using tail DNA. PCR primers were: loxP-F (5′-CGAAGTTATGGATCCCGGACC-3′) and Cα4-R (5′-AAGAAGGAGCGGAGGGGTGAG-3′) for Cα^{fl} (94°C for 30 s, 62°C for 30 s, and 72°C for 30 s; 333 bp); Cα E1-F (5′-CCAAATCAATGTGCCGAAAAC-3′) and pGKprom -R (5′-TACCCGCTTCCATTGCTCAG-3′) for TCR$\alpha^{-/-}$ (94°C for 30 s, 59°C for 30 s, and 72°C for 30 s; 424 bp); and Mx-Cre F (5′-CATGTGTCTTGGTGGGCTGAG-3′) and Mx-Cre R (5′-CGCATAACCAGTGAAACAGCAT-3′) for the Mx-Cre transgene (94°C for 30 s, 54°C for 45 s, and 72°C for 45 s; 596 bp).

Plasmids, Hybridization Probes, and Targeting Vector. The targeting vector pTCRα flox 1 was constructed by subcloning of the Jα and Cα elements from a TCR shuttle vector (kindly provided by Mark Davis, Stanford University, Stanford, CA) into the plasmid pEasy Flox generated and kindly provided by Marat Alimzhanov, Institute for Genetics, University of Cologne, Cologne, and containing the selection marker genes HSV-TK and pGK neo and three lox P sites. Specifically, a *Nde*I-*Bam*HI fragment containing the first four Jα elements and part of the Jα-Cα intron was subcloned into a *Hin*dIII site downstream of the HSV-TK, and a *Bam*HI–*Bsp*EI fragment containing the Cα4 exon into a *Bam*HI site, downstream of the loxP-flanked neo gene of pEasy Flox. A Cα1-Cα3 containing the *Bam*HI–*Xho*I fragment, previously subcloned from the TCRα shuttle vector into pBluescript KS+, was cloned into the *Sal*I site between two loxP sites of pEasy Flox.

External probe A, complementary to the Jα6 element, and probe B, complementary to the TCRα enhancer, were used for hybridization of *Bam*HI and *Hin*dIII or *Eco*RI digested genomic DNA, respectively, to identify homologous recombinants. Cointegration of the third loxP site was determined by using probe A and *Bam*HI digestion (Fig. 1*a*). Probe C, an *Rsr*II–*Pst*I fragment of the neo cassette, was used as internal probe to identify random integrants.

Embryonic Stem (ES) Cells, Gene Targeting, and Blastocyst Injection. Bruce 4 ES cells of C57BL/6 origin and feeder cells were grown under conditions described previously (13). ES (10^7) cells were transfected with 30 μg linearized (*Not*I) pTCRα flox vector. Selected colonies were picked on day 10 after transfection and screened for homologous recombinants by Southern blot analysis. Homologous recombinants were transiently transfected with a Cre-encoding plasmid, as described previously (13). Two neo-deleted subclones were injected into CB-20-derived blastocysts, which were subsequently transferred into (C57BL/6 × BALB/c) F_1 foster mothers. From each injected clone, we obtained several chimeras, which we bred to C57BL/6 mice.

Abbreviations: MHC, major histocompatibility complex; BCR, B cell antigen receptor; TCR, T cell antigen receptor; CFDA-SE, carboxyfluorescein diacetate–succinimidyl ester; pI/pC, poly(I)-poly(C); ES, embryonic stem.

‡To whom reprint requests should be addressed. E-mail: bojanp@medri.hr (B.P.) or kr@mac.genetik.uni-koeln.de (K.R.).

The publication costs of this article were defrayed in part by page charge payment. This article must therefore be hereby marked "*advertisement*" in accordance with 18 U.S.C. §1734 solely to indicate this fact.

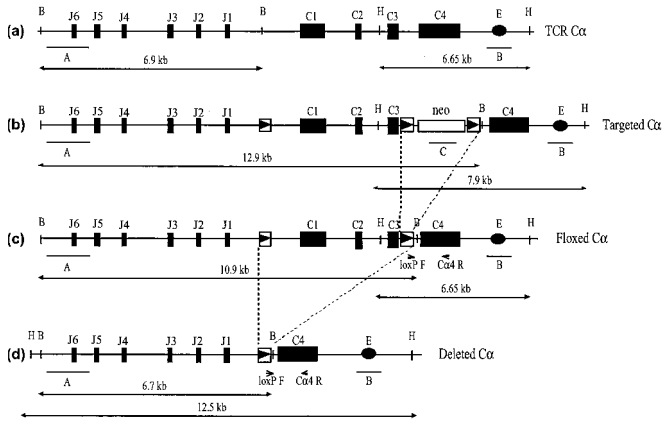

Fig. 1. Targeting of the TCR Ca locus. (*a*) Partial restriction map of the TCR Ca locus. Restriction sites for *Bam*HI (B) and *Hin*dIII (H) endonuclases are shown. Jα elements and Cα exons are depicted as closed squares and the TCRα enhancer, as a closed circle. External hybridization probes A and B, used to verify homologous recombination of the targeting vector by Southern blot, together with expected sizes of the DNA fragments, are indicated below the line. (*b*) Targeted TCR Cα locus. LoxP sites, framed closed triangles; neo cassette, dotted square. Introduction of the loxP site in the Jα-Cα intron caused destruction of a *Bam*HI site, which was used to determine homologous recombination and third loxP cointegration by probe A. Probe C was used to exclude random integration of the vector. (*c*) Conditional Cα allele after deletion of the neo cassette by transient expression of Cre recombinase in targeted ES cells. Small arrows show PCR primers (loxP F and Cα4 R) designed for detection of the loxP-flanked Cα allele. (*d*) Deletion of TCR Cα genes after induction of Cre expression *in vivo*.

Germ-line transmission of the targeted TCR Cα allele was obtained for both ES cell clones.

Immunofluorescence and Flow Cytometry. The following reagents were used for immunofluorescence staining: FITC, phycoerythrin (PE), Cychrome (Cye), or APC-conjugated mAbs to: CD4 (GK 1.5, in house), CD8 (53.6.7, in house), TCRβ, CD3ε, CD5, B220, CD62L, CD69, and Ly6C (PharMingen); Streptavidin–PE (Southern Biotechnology Associates); Streptavidin-Cyc (PharMingen); and Streptavidin-Cy7 PE (Caltag, South San Francisco, CA). Spleen or lymph node cells were stained in PBS containing 2% BSA and 0.2% of NaN_3 and analyzed on a FACS Calibur by using CELLQUEST software (Becton Dickinson). To increase sensitivity of TCRβ staining, we used magnetofluorescent liposomes, as described previously (14–16). Briefly, cells were incubated with FITC-conjugated anti-TCRβ mAbs (PharMingen) followed by digoxigenin (DIG)-conjugated anti-FITC mAbs and, finally, anti-DIG mAbs coupled with magnetofluorescent liposomes.

BrdUrd Labeling and Analysis of T Cell Proliferation *in Vivo*. The proliferative activity of T cells *in vivo* was determined by BrdUrd labeling as described previously (17). Briefly, BrdU (Sigma, B-5002) was added to the drinking water (1 mg/ml) of the experimental animals for 7 days before flowcytometric analysis of the cells. TCR^+ and TCR^- subsets of $CD4^+$ and $CD8^+$ T cells from the spleen were sorted on a FACStar (Becton Dickinson) and subsequently stained for CD44 by using biotinylated mAb (PharMingen). After fixation, the cells were resuspended in 2 M HCl containing 0.5% Tween-20 and then stained with FITC-conjugated anti-BrdU mAb (Becton Dickinson), followed by Streptavidin-Cyc (PharMingen).

Proliferation Assays

Proliferation of T Cells on Crosslinking of the TCR. Spleen cells from $C\alpha^{fl/-}$, Mx-Cre mice, isolated 12 days after the poly(I)-poly(C) (pI/pC) injection, were stained for CD4, CD8, and TCRβ. TCR^+ and TCR^- subsets of either $CD4^+$ or $CD8^+$ T cells were sorted on a FACStar (Becton Dickinson) and subsequently used in the proliferation assays. Briefly, 96-well plates were coated with either anti-CD3ε (PharMingen) or anti-TCRβ (PharMingen) mAbs (20 μg/ml) in PBS at 37°C for 2 h. Sorted subsets of cells were labeled with 2 μM 5- (and 6-) carboxyfluorescein diacetate, succinimidyl ester (CFDA-SE) (Molecular Probes) in PBS for 5 min at 37°C and subsequently added to the coated plates (2×10^5 cells/well) in RPMI medium 1640 (GIBCO/BRL) containing 10% FCS. After 72 h, the cells were stained for CD4, CD8, and TCRβ and analyzed on a FACS Calibur (Becton Dickinson).

IL-15 Assay. Splenic T cells from the experimental mice were magnetically sorted according to CD4 and CD8 expression by using the midi-MACS system (Miltenyi Biotec, Auburn, CA). The cells were labeled with CFDA-SE (see above) and subsequently plated on 96-well plates (2×10^5 cells/well) in RPMI 1640 containing 10% FCS. Human recombinant IL-15 (R & D Systems) was added at various concentrations, and after 72 h of incubation, the cells were stained for CD4 or CD8, TCRβ, and CD44, and analyzed by flow cytometry.

Calcium Flux Analysis. Spleen (10^7) or lymph node cells, isolated 12 days after pI/pC injection, were loaded with the Ca^{2+}-sensitive dye Indo-1 (2 μM, Molecular Probes) in 1 ml of RPMI 1640 containing 5% FCS at 37°C for 30 min and subsequently stained with FITC-conjugated mAbs to CD4 or CD8 and a saturating concentration (10 μg/ml) of phycoerythrin-conjugated mAbs to either CD3ε (145–2C11, PharMingen) or TCRβ (H57–597, PharMingen). Calcium flux was induced by crosslinking of either anti-CD3ε or anti-TCRβ mAbs by adding to the sample goat anti-hamster Ab (10 μg/ml, Cappel) 50 s after the beginning of the analysis. Light emission was recorded at 395 and 530 nm, and the ratio between the two emissions was used as a readout for relative calcium concentrations.

Reverse Transcription–PCR Analysis of pTα Expression. Total RNA was isolated from sorted TCR^+ and TCR^- subsets of $CD4^+$ and $CD8^+$ splenic T cells and, as a positive control, from DP thymocytes of the experimental and TCR$\alpha^{-/-}$ mice. Briefly, 1.6×10^6 cells were lysed in Trizol (GIBCO/BRL), and RNA was extracted according to the manufacturer's protocol. cDNA was prepared by using random hexamer primers (Roche Diagnostics) and Superscript (GIBCO/BRL). Exon spanning primers and PCR conditions for amplification of pTα and β-actin have been described previously (18, 19). PCR products were analyzed after 18, 21, 24, 27, and 30 cycles. They were visualized by Southern blotting by using oligonucleotide probes for pTα (5′CAGGTACTGTGGCTGAGCCTACTG3–3′ (18), and β-actin (5′GTGGGCCGCTCTAGGCACCAA3′) for hybridization.

Results

Targeting of the TCR Cα Locus. The targeting vector contained the four downstream Jα elements (J1–J4) and the four exons (C1–C4) of the Cα gene segment. A loxP-flanked neomycin resistance (neo) gene was inserted into the intron between C3 and C4, and a single loxP site upstream of C1. The wild-type TCR Cα locus (*a*) and the locus on homologous recombination with the targeting vector (*b*) are depicted in Fig. 1. Cre-mediated deletion of the neo gene in the recombinant ES cells generated the desired conditional Cα allele ($C\alpha^{fl}$, *c*) from which a Cα null allele can be obtained through Cre-mediated recombination (*d*). Homologous recombinants were identified through gene amplification by PCR and confirmed by Southern blotting, as was deletion of the neo gene (data not shown). The $C\alpha^{fl}$ allele was subsequently transmitted into the mouse germ line (data not shown; see Fig. 2*C*).

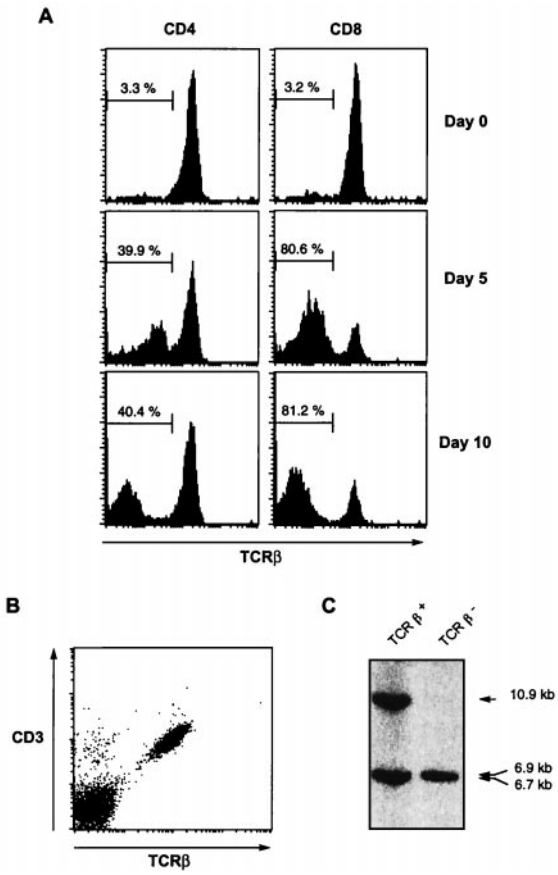

Fig. 2. (*A*) Decay of TCR from T cells upon conditional Cα deletion. Flow cytometric determination of TCRβ expression on CD4$^+$ (*Left*) and CD8$^+$ (*Right*) peripheral blood T cells. Days after the injection of pI/pC and percentages of T cells with down-regulated TCRβ are indicated. (*B*) Simultaneous decay of CD3 complex with TCRβ on Cα-deleted T cells. Dot plot represents CD5-gated peripheral blood lymphocytes on day 15 after injection of pI/pC. Cells were analyzed for surface CD3ε and TCRβ expression by flow cytometry. (*C*) Southern blot analysis of TCR$^+$ and TCR$^-$ T cells. TCR$^+$ and TCR$^-$ subsets of CD4$^+$ and CD8$^+$ T cells isolated from the spleen of C$\alpha^{fl/-}$ mice 10 days after the injection of pI/pC were sorted, and genomic DNA was analyzed for Cα deletion. *Bam*HI-digested DNA was hybridized with probe A (see Fig. 1*A*). Bands indicate TCR$\alpha^{-/-}$ (6.9 kb), Cα-deleted (Cα^{Δ}, 6.7 kb), and Cα^{fl} (10.9 kb) alleles.

Decay of TCR on T Cells on Induced Cα Deletion. To induce loss of TCR in mature T cells, we generated mice that carried the Cα^{fl} allele on one chromosome and a Cα null allele (11) on the other, together with the Mx-Cre transgene from which Cre is expressed on induction with type I IFN (IFN I) or its inducer pI/pC (10). These mice produced normal numbers of T cells expressing TCR$\alpha\beta$ at wild-type levels (data not shown). At the age of 6 wk, the animals were given a single dose (400 μg) of pI/pC and were bled or killed at various times thereafter, to determine the extent of TCR deletion and its effect on the corresponding cells. pI/pC-treated C$\alpha^{+/-}$, Mx-Cre, and C$\alpha^{fl/-}$ mice served as controls.

As shown in Fig. 2*A*, down-regulation of TCRβ could be observed as early as 5 days after pI/pC treatment on a fraction of CD4$^+$ (40%) and CD8$^+$ (80%) T cells in the blood. On day 10, the affected cells were negative for TCRβ and CD3ε (Fig. 2*B*) by conventional staining, indicating that they had largely lost the TCR$\alpha\beta$/CD3 complex from the cell surface, while fully retaining CD4 or CD8 expression. These cells had indeed undergone TCRα deletion, in contrast to the TCRβ^+ cells (Fig. 2*C*).

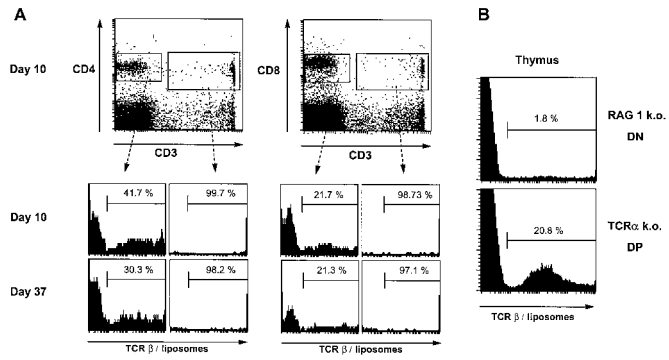

Fig. 3. (*A*) Persistence of low levels of TCR on the surface of T cells upon Cα deletion. CD3$^+$ and CD3$^-$ fractions of CD4$^+$ and CD8$^+$ T cells were analyzed for TCRβ expression by staining with an anti-TCRβ mAb and magnetofluorescent liposomes. Dot plots show gated fractions of CD4$^+$ (*Left*) and CD8$^+$ (*Right*) peripheral blood T cells. Histograms below show expression of TCRβ by liposome staining on gated fractions of T cells. Percentages of TCRβ-positive cells and time of analysis are indicated. (*B*) Sensitivity of liposome-assisted staining for TCRβ. Sensitivity of liposome staining for TCRβ was tested on CD4$^+$ CD8$^+$ TCR$\alpha^{-/-}$ thymocytes. Data are represented as histograms, and percentages of TCRβ^+ cells are indicated. Staining of thymocytes from RAG1-deficient mice, as a negative control, shows background of the liposome-assisted staining.

Persistence of Low-Level TCRβ Expression on the Surface of Cα-Deficient T Cells. Are the TCR-negative cells as depicted in Fig. 2 *A* and *B* fully devoid of TCR? Although the staining of these cells was 2.5–3 orders of magnitude below that of wild-type cells, indicating loss of the vast majority of TCR complexes from the cell surface, conventional staining methods do not permit the detection of a small number of such complexes that might persist on the cell surface for extended periods of time. We therefore used a more sensitive staining method that makes use of antibodies conjugated to magnetofluorescent liposomes, increases sensitivity by 1–2 orders of magnitude, and has previously allowed the detection of membrane-bound proteins, which are below, or just at, the limit of detection by standard methods (15, 16).

Peripheral blood T cells were stained by standard methods for CD4, CD8, and CD3ε, and for expression of TCRβ with an anti-TCRβ antibody and magnetofluorescent liposomes at days 0, 6, 10, 37, and 49 after pI/pC injection. Results are shown in Fig. 3*A* for the time points 10 and 37 days (the results obtained on day 49 are similar to the latter). As expected, all CD4$^+$ and CD8$^+$ cells positive for CD3 by conventional staining were strongly stained in the magnetofluorescence assay. Surprisingly, however, we also found some liposome-stained cells in the CD3-negative fractions of both CD4$^+$ and CD8$^+$ cells. At day 37, the fraction of these cells, on which no TCRβ could be detected by conventional staining, ranged between 20 and 30% (Fig. 3*A Bottom*). Staining appeared to be specific, as it was not observed on thymocytes of RAG1-deficient mice (Fig. 3*B Upper*) and resembled TCRβ staining on TCRα-deficient, CD4$^+$ CD8$^+$ thymocytes (Fig. 3*B Lower*). However, the TCRα-deficient cells did not contain detectable mRNA for the pTα chain as assessed by reverse transcription–PCR and are thus unlikely to express pre-TCR (data not shown; see also *Materials and Methods*). At low levels of antigen expression (in the range of 100 molecules per cell), liposome-based staining is no longer quantitative in that only a fraction of the cells may be hit by a liposome-conjugated antibody (15). The staining data in Fig. 3 thus indicate that on induced TCR Cα deletion, most or all peripheral T cells retain a small number of TCR$\alpha\beta$ complexes or TCRβ chains complexed to some other protein(s) on their surface, whereas the vast majority of the receptor complexes disappear

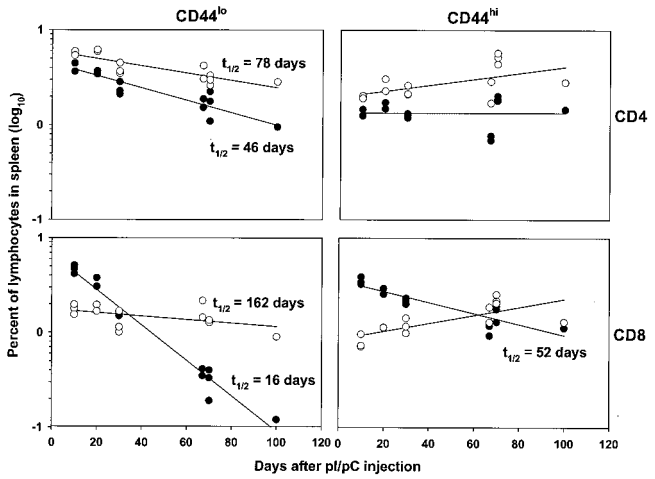

Fig. 4. Decay of T cells upon TCR Cα deletion. Percentages of CD44^{lo} (*Left*) and CD44^{hi} (*Right*) CD4$^+$ (*Upper*) and CD8$^+$ cells (*Lower*) in the spleens of the experimental animals at various times after pI/pC injection. Open circles, TCR$^+$ cells; closed circles, TCR$^-$ cells. Experimental points come from individual animals. Half-lives ($t_{1/2}$) were calculated from regression lines (SIGMA PLOT program, Ver. 4.0, SPSS, Chicago).

within a few days. For simplicity, we designate these cells as TCR$^-$ cells below.

Decay of TCR$^-$ T Cells Over Time. Three weeks after induction of TCRα deletion by pI/pC, we found the thymi of the experimental animals devoid of CD4$^+$ or CD8$^+$ "single-positive" T cells (data not shown). This is expected, given that Cre-mediated recombination in this system is complete in lymphoid progenitors, as we have observed for several loxP-flanked gene segments. Thus, we could follow in the experimental animals the decay of TCR$^+$ and TCR$^-$ T cells over time, in the absence of cellular influx from the thymus.

In Fig. 4, we plot the percentages of TCR$^+$ and TCR$^-$ CD4$^+$ and CD8$^+$ cells against time, separated into naïve and memory/activated T cells on the basis of the expression of the CD44 surface marker. The results differed dramatically for the various T cell subsets. In the case of the naïve (CD44^{lo}) cells, a rapid decay was observed for the TCR$^-$ CD8$^+$ cells, the percentages of their TCR$^+$ counterparts being essentially stable over time. In the CD4$^+$ compartment, the percentages of the TCR$^-$ cells also declined, but much more slowly, and some decline was also seen for the TCR$^+$ cells. As the data nicely fitted linear regression lines in the half-logarithmic plot, we could calculate half-lives for the various cellular subsets, namely TCR$^-$ CD8$^+$ naïve cells ($t_{1/2} \approx 16$ days), TCR$^+$, CD8$^+$ naïve cells ($t_{1/2} \approx 162$ days), TCR$^-$, CD4$^+$ naïve cells ($t_{1/2} \approx 46$ days), and TCR$^+$, CD4$^+$ naïve cells ($t_{1/2} \approx 78$ days). Virtually identical results were obtained when absolute cell numbers were plotted against time, as the absolute numbers of splenic lymphocytes did not significantly change over the time of observation (data not shown). In the compartments of CD4$^+$ and CD8$^+$ memory (CD44^{hi}) cells, percentages of TCR$^+$ cells increased over time, strongly in the case of CD4$^+$ and moderately in that of CD8$^+$ cells, reflecting, perhaps, homeostatic cellular expansion in a situation in which TCR$^-$ naïve cells were progressively lost. Such an expansion has been described earlier and can be associated with a change to a memory phenotype (21–23). A similar increase was not seen for the percentages of TCR$^-$ cells of memory phenotype: the TCR$^-$ CD4$^+$ cells persisted at constant levels, and their CD8$^+$ counterparts declined slowly ($t_{1/2} \approx 52$ days). As shown further below (Fig. 5), these results correlate with a more pronounced proliferative activity of the TCR$^+$ memory cells, as compared with their TCR$^-$ counterparts.

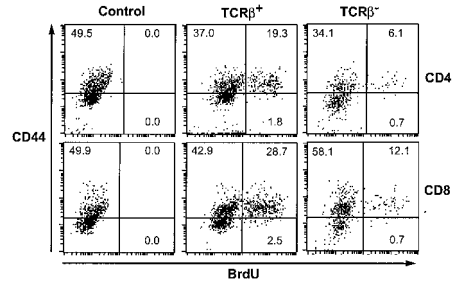

Fig. 5. Proliferation of TCR$^-$ memory T cells. C$\alpha^{fl/-}$, Mx-Cre, and C$\alpha^{fl/-}$ mice were fed with BrdU containing drinking water from day 60 to 67 after pI/pC injection. Controls did not receive BrdU. TCR$^+$ and TCR$^-$ subsets of CD4$^+$ and CD8$^+$ T cells were then sorted and stained for CD44 and BrdU. Percentages of cells in various subpopulations are indicated.

The more rapid clearance of the CD44^{lo} naïve cells could also be seen when the cells are costained for the expression CD62L, a typical marker of naïve T cells (Fig. 7, which is published as supplemental data on the PNAS web site, www.pnas.org), and of Ly6C, which is expressed on memory but not naïve T cells (ref. 30; supplemental data). As expected, the TCR$^-$, CD44^{lo} naïve cells essentially lacked expression of the activation marker CD69, which was expressed, however, on a small fraction of the CD44^{hi}, CD8$^+$ cells and a substantial fraction of the CD44^{hi}, CD4$^+$ cells (supplemental data).

Properties of TCR$^-$ Cells. Overall, the TCR$^-$ cells differed from their TCR$^+$ counterparts in the expression of two membrane proteins, which are known to be of physiological relevance for the cells, namely CD5, which was down-regulated (supplemental data, www.pnas.org), and the Fas receptor, which was slightly up-regulated on the cells throughout the period of observation (data not shown). CD5 down-regulation may reflect an adaptive response of the cells to decrease signaling thresholds (24) when the level of TCR expression decreases. Whether Fas up-regulation contributes to the elimination of the receptorless cells remains an open question.

To clarify whether the decay rates measured for the various T cell subsets on TCR ablation are affected by cell proliferation, we assessed the proliferative activity of the TCR$^+$ and TCR$^-$ CD4$^+$ and CD8$^+$ cells by feeding experimental animals with BrdU for 7 days, starting on day 60 after pI/pC treatment (Fig. 5). No BrdU incorporation was detected in CD44^{lo} cells, irrespective of TCR expression. In contrast, 34% of the TCR$^+$, CD4$^+$, and 40% of the TCR$^+$, CD8$^+$ cells expressing CD44 incorporated BrdU within the 7 days of feeding. In the CD44^{hi}, TCR$^-$ cells, BrdU incorporation was also seen, but the fraction of labeled cells was substantially smaller (15 and 17%, respectively).

Do the residual TCRβ chains on the surface of TCR$^-$ cells allow cellular activation on crosslinking? We compared activation of TCR$^+$ and TCR$^-$ CD4$^+$ and CD8$^+$ cells by anti-TCRβ and anti-CD3ε antibodies. As can be seen from Fig. 6, the TCR$^+$ cells responded to both stimuli by vigorous proliferation (Fig. 6*A*) and showed the typical wave of Ca^{2+} mobilization on CD3ε (Fig. 6*B*) and TCRβ crosslinking (data not shown). Neither response was observed in the case of the TCR$^-$ cells.

Finally, we asked whether the sensitivity of CD8$^+$ memory T cells to their growth factor IL-15 (25) would be maintained by the cells after TCR ablation. The data depicted in Fig. 6*C* show this is clearly the case, although the proliferative response of the TCR$^-$ cells may be slightly reduced as compared with that of their TCR$^+$ counterparts. As expected, naive (CD44^{lo}) CD8$^+$

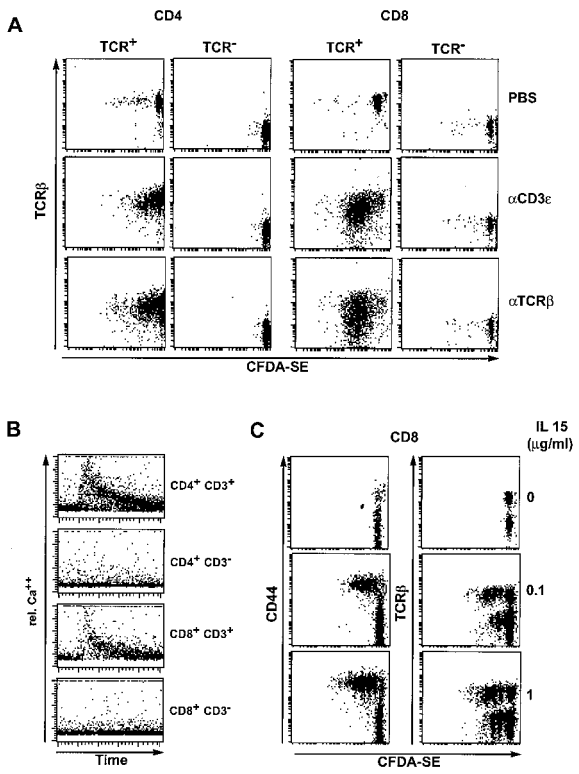

Fig. 6. Functional properties of TCR$^-$ T cells. (*A*) Lack of proliferation on TCR crosslinking *in vitro*. FACS-sorted TCR$^+$ and TCR$^-$ subsets of CD4$^+$ and CD8$^+$ splenic T cells, isolated on day 10 after pI/pC injection, were labeled with CFDA-SE, incubated in the presence of either anti-CD3ε or anti-TCRβ plate-bound mAbs for 72 h, and subsequently analyzed by flow cytometry. (*B*) Lack of Ca^{2+} mobilization on CD3ε crosslinking. Spleen cells were isolated on day 12 after pI/pC injection, loaded with the Ca^{2+}-sensitive dye Indo-1, and subsequently stained for CD4 or CD8 and CD3e. Relative intracellular Ca^{2+} concentration was measured on gated CD3ε^+ and CD3ε^- T cells during the time period of 512 s. (*C*) Proliferation of TCR$^-$ CD8$^+$ memory T cells on stimulation with IL-15. Magnetically sorted and CFDA-SE-labeled splenic CD8$^+$ T cells were incubated for 72 h in the presence of human recombinant IL-15 at various concentrations, as indicated. Subsequently, the cells were stained for CD8, TCRβ, and CD44 and analyzed by flow cytometry.

cells do not respond to IL-15. We also tested CD4$^+$ cells in this assay and, in accord with Zhang *et al.* (25), found no response in the case of the naive and a marginal response in that of the memory cells, irrespective of TCR expression (data not shown).

Discussion

We have established a system of TCR$\alpha\beta$ ablation by combining the IFN-inducible Mx-Cre transgene with a loxP-flanked TCR Cα gene together with a TCRα null allele. pI/pC injection leads to the deletion of Cα in 40% of peripheral mature CD4$^+$ and 80% of CD8$^+$ cells. After about 10 days, the level of expression of the TCR complex on the surface of the Cα-deficient cells has declined by 2.5–3 orders of magnitude, as assessed by staining for TCRβ and CD3. Assuming that staining intensity is roughly proportional to the number of surface-bound TCR complexes, and that about 30,000 such complexes are expressed on mature T cells (26, 27), we conclude that no more than 100 TCR complexes could be expressed on the surface of the Cα-deficient cells 10 days after induction of Cα deletion. To our surprise, we found that, on the basis of liposome-assisted flow cytometric analysis, low levels of TCRβ chains, likely in the order of 100 molecules per cell when we take analogous data from the literature into account (15), were indeed detectable not only on day 10 but also up to at least 7 weeks after Cα deletion. We do not know at present whether this reflects the presence of a small fraction of TCR$\alpha\beta$ complexes on the cell surface that are not subject to turnover or TCRβ expression in conjunction with some other molecule, which is, however, not the pTα chain (28, 29). Because we have been unable to obtain any detectable cellular activation on exposure of the cells to anti-TCRβ or -CD3ε antibodies and also find an essentially complete block of thymic CD4$^+$ and CD8$^+$ T cell production on pI/pC treatment, we consider the cells from day 10 after Cα deletion as TCR deficient in functional terms and designate them as TCR$^-$.

From day 10, the receptorless naive T cells in spleen (Fig. 4), blood, and lymph nodes (data not shown) begin to decay, the decay being more rapid for CD8$^+$ than for CD4$^+$ cells. In contrast to the TCR$^-$ cells, their TCR$^+$ counterparts remained constant in number or declined more slowly over the time of observation, even though from 3 weeks after pI/pC injection, the thymi of the animals were essentially devoid of CD4$^+$ and CD8$^+$ T cells, because of efficient TCR Cα deletion in lymphoid progenitors. Thus, the TCR$^-$ naive cells were selectively lost, but this selectivity was much more pronounced in the CD8$^+$ than in the CD4$^+$ compartment. Although we cannot exclude that the loss of naive cells in part reflects interconversion of naive to memory T cells, triggered perhaps by pI/pC-induced IFN, we consider it unlikely that this represents a major effect. Indeed, we have not observed a significant change in the proportions of naive versus memory TCR$^+$ cells 10 days after pI/pC injection, and earlier work has shown that IFN-induced up-regulation of CD44 and Ly6C on naive T cells is transitory and not accompanied by cellular proliferation (30, 31).

How do the rates of decay of receptorless naïve T cells compare with those determined for T cells exposed to an environment free of appropriate MHC ligands? The half-life of 46 days determined for the population of naive TCR$^-$, CD4$^+$ cells in the present study is very similar to that reported in two independent studies for naive CD4$^+$ cells in a nonmatching MHC environment (50 and 42 days, respectively; refs. 3 and 4). However, taking cell proliferation into account, Rooke *et al.* calculate a true half-life of the cells of 26 days, a result later confirmed by the same group by using a different approach (3, 5). As we do not observe significant cell proliferation in the naive receptorless cells, it would follow that naive CD4$^+$ T cells expressing an intact TCR but unable to interact with MHC would thus seem to die somewhat faster than the same cells on induced TCR ablation—an apparently paradoxical conclusion. We rather believe that the true decay rate of receptorless naive CD4 cells is similar to that of TCR competent cells that are not "tickled" by MHC antigens, and that the differences between decay rates are due to differences between the experimental systems. Thus, T cell life spans are known to be different in the presence and absence of cellular influx from the thymus (20). In naive CD8$^+$ cells, TCR ablation leads to a more rapid loss of the cells, with a calculated half-life of just a little over 2 weeks. Rapid cell loss has also been reported for such cells when transferred to an MHC-inappropriate environment, starting either on cell transfer (7) or after initial cellular expansion (6). Decay rates in these cell transfer systems were either more rapid than in the present study (7) or roughly comparable (6).

Altogether, the results are compatible with the concept that the TCR contributes to the maintenance of naive T cells mainly on the basis of TCR–MHC ligand interaction and not a TCR-autonomous "maintenance" signal, as might be delivered to B cells through the BCR (1, 32)

In the case of memory T cells, the present data support the general conclusion from earlier work that these cells depend less on TCR–MHC ligand interaction than do naive T cells (6–9). We found no decline of receptorless CD4$^+$ memory cells, and the decay rate of TCR$^-$ CD8$^+$ memory cells was much slower than that of their naive counterparts (52 versus 16 days). Both TCR$^+$

and TCR^- $CD8^+$ memory cells (but not naive $CD8^+$ cells) responded to IL-15 by vigorous proliferation, supporting the concept that this lymphokine plays a dominant role in the maintenance of these cells (25) and directly demonstrating that their response to IL-15 is, at least in a first approximation, independent of TCR expression. In accord with the work of Zhang *et al.* (25), IL-15 had only little effect on TCR^+ or TCR^- $CD4^+$ cells, whose maintenance must thus be controlled by some other factor(s).

Whether TCR–MHC ligand interaction also contributes to the maintenance of memory T cells has been controversial, although it seems clear that, as in the case of memory B cells (33), recognition of (MHC-bound) antigen is not required (6–9). Considering only cellular decay, the present data argue against a role of TCR–MHC interaction in the maintenance of $CD4^+$ memory cells, supporting the earlier work of Swain *et al.* (8, 9), and demonstrate a role for the TCR in the maintenance of $CD8^+$ memory cells. The latter could reflect the dependence of (some of) the cells on TCR interaction with low-affinity ligands in the environment (7). However, the interpretation of the data is complicated by the fact that, in contrast to the naive cells, memory T cells exhibit substantial proliferative activity that is more pronounced in TCR^+ compared with TCR^- cells (Fig. 5). Thus, cellular proliferation contributes to the maintenance of memory T cells (34, 35) and led in the present system to an expansion of TCR^+ cells in both the $CD4^+$ and the $CD8^+$ compartments. Therefore, taking both cellular decay and expansion into account, receptorless $CD4^+$ and $CD8^+$ memory cells were both at a disadvantage against their TCR^+ counterparts *in vivo*.

Comparing B and T cell physiology, ablation of antigen receptor expression on naive B and T cells leads to the disappearance of the cells in all cases, but the kinetics of decay differ for different classes of cells. Although TCR and BCR appear to be lost from the cell surface at roughly similar rates (ref. 1 and present data), rates of cellular decay are most rapid for B cells (1), intermediate for $CD8^+$, and slow for $CD4^+$ cells. B cells seem to die by apoptosis as soon as the level of BCR expression reaches a certain threshold (1). In contrast, T cells that are essentially TCR^- can be observed in experimental animals over prolonged periods of time. Curiously, these cells maintain surface expression of TCRβ chains at very low levels. Although we have been unable to activate such cells by anti-TCRβ or anti-CD3ε antibodies, induced TCRβ ablation will be required to definitively demonstrate whether these residual molecular complexes of unknown structure affect cellular survival.

Apart from this possibility, we see no reason from the present data to suspect that spontaneous signaling by the $\alpha\beta$TCR plays a significant role in T cell homeostasis. Indeed, the evidence is strongly against such a possibility, in that T cells apparently tolerate the loss of TCR expression as such. Such a case cannot be made for naive B cells, which rapidly undergo apoptosis when BCR expression falls below a certain threshold. This may reflect the dependence of these cells on a BCR-autonomous ligand-independent maintenance signal and thus a fundamental difference between the homeostasis of naive B and T cells.

We thank Drs. H. v. Boehmer, T. Buch, I. Foerster, M. Alimzhanov, and S. Casola for discussion, Drs. M. Alimzhanov and M. Davis for gifts of plasmids, and C. Goettlinger, A. Roth, and A. Egert for technical help. This work was supported by the Deutsche Forschungsgemeinschaft through SFB243, the Koerber Foundation, the European Union (Grant QLG1-1999-00202), and an A. v. Humboldt Foundation fellowship to B.P.

1. Lam, K. P., Kuhn, R. & Rajewsky, K. (1997) *Cell* **90,** 1073–1083.
2. Kirberg, J., Berns, A. & von Boehmer, H. (1997) *J. Exp. Med.* **186,** 1269–1275.
3. Rooke, R., Waltzinger, C., Benoist, C. & Mathis, D. (1997) *Immunity* **7,** 123–134.
4. Takeda, S., Rodewald, H. R., Arakawa, H., Bluethmann, H. & Shimizu, T. (1996) *Immunity* **5,** 217–228.
5. Witherden, D., van Oers, N., Waltzinger, C., Weiss, A., Benoist, C. & Mathis, D. (2000) *J. Exp. Med.* **191,** 355–364.
6. Murali-Krishna, K., Lau, L. L., Sambhara, S., Lemonnier, F., Altman, J. & Ahmed, R. (1999) *Science* **286,** 1377–1381.
7. Tanchot, C., Lemonnier, F. A., Perarnau, B., Freitas, A. A. & Rocha, B. (1997) *Science* **276,** 2057–2062.
8. Swain, S. L. (2000) *Philos. Trans. R. Soc. London B Biol. Sci.* **355,** 407–411.
9. Swain, S. L., Hu, H. & Huston, G. (1999) *Science* **286,** 1381–1383.
10. Kuhn, R., Schwenk, F., Aguet, M. & Rajewsky, K. (1995) *Science* **269,** 1427–1429.
11. Mombaerts, P., Clarke, A. R., Rudnicki, M. A., Iacomini, J., Itohara, S., Lafaille, J. J., Wang, L., Ichikawa, Y., Jaenisch, R., Hooper, M. L., *et al*. (1992) *Nature (London)* **360,** 225–231.
12. Mombaerts, P., Iacomini, J., Johnson, R. S., Herrup, K., Tonegawa, S. & Papaioannou, V. E. (1992) *Cell* **68,** 869–877.
13. Torres, R. M. & Kühn, R. (1997) *Laboratory Protocols for Conditional Gene Targeting* (Oxford Univ. Press, Oxford, U.K.).
14. Scheffold, A., Miltenyi, S. & Radbruch, A. (1995) *Immunotechnology* **1,** 127–137.
15. Scheffold, A., Assenmacher, M., Reiners-Schramm, L., Lauster, R. & Radbruch, A. (2000) *Nat. Med.* **6,** 107–110.
16. Bruno, L., Scheffold, A., Radbruch, A. & Owen, M. J. (1999) *Curr. Biol.* **9,** 559–568.
17. Tough, D. F. & Sprent, J. (1994) *J. Exp. Med.* **179,** 1127–1135.
18. Bruno, L., Rocha, B., Rolink, A., von Boehmer, H. & Rodewald, H. R. (1995) *Eur. J. Immunol.* **25,** 1877–1882.
19. Trop, S., Rhodes, M., Wiest, D. L., Hugo, P. & Zuniga-Pflucker, J. C. (2000) *J. Immunol.* **165,** 5566–5572.
20. von Boehmer, H. & Hafen, K. (1993) *J. Exp. Med.* **177,** 891–896.
21. Goldrath, A. W., Bogatzki, L. Y. & Bevan, M. J. (2000) *J. Exp. Med.* **192,** 557–564.
22. Cho, B. K., Rao, V. P., Ge, Q., Eisen, H. N. & Chen, J. (2000) *J. Exp. Med.* **192,** 549–556.
23. Kieper, W. C. & Jameson, S. C. (1999) *Proc. Natl. Acad. Sci. USA* **96,** 13306–13311.
24. Pena-Rossi, C., Zuckerman, L. A., Strong, J., Kwan, J., Ferris, W., Chan, S., Tarakhovsky, A., Beyers, A. D. & Killeen, N. (1999) *J. Immunol.* **163,** 6494–6501.
25. Zhang, X., Sun, S., Hwang, I., Tough, D. F. & Sprent, J. (1998) *Immunity* **8,** 591–599.
26. Allison, J. P., McIntyre, B. W. & Bloch, D. (1982) *J. Immunol.* **129,** 2293–2300.
27. Janeway, C. (1999) *Immunobiology: The Immune System in Health and Disease* (Garland, London).
28. Bruno, L., Kirberg, J. & von Boehmer, H. (1995) *Immunity* **2,** 37–43.
29. Barber, D. F., Passoni, L., Wen, L., Geng, L. & Hayday, A. C. (1998) *J. Immunol.* **161,** 11–16.
30. Dumont, F. J. & Coker, L. Z. (1986) *Eur. J. Immunol.* **16,** 735–740.
31. Tough, D. F., Borrow, P. & Sprent, J. (1996) *Science* **272,** 1947–1950.
32. Neuberger, M. S. (1997) *Cell* **90,** 971–973.
33. Maruyama, M., Lam, K. P. & Rajewsky, K. (2000) *Nature (London)* **407,** 636–642.
34. Clarke, S. R. & Rudensky, A. Y. (2000) *J. Immunol.* **165,** 2458–2464.
35. Dorfman, J. R., Stefanova, I., Yasumoto, K. & Germain, R. N. (2001) *Nat. Immunol.* **2,** 136–137.